European Rotorcraft Forum

AERODYNAMIC ANALYSIS OF HELICOPTER IN INTERACTION WITH WIND TURBINE'S WAKE

Theologos E. Andronikos, theologos@fluid.mech.ntua.gr, National Technical University of Athens, School of Mechanical Engineering (Greece)

George Papadakis, papis@fluid.mech.ntua.gr, National Technical University of Athens, School of Naval Architecture & Marine Engineering (Greece)

Vasilis Riziotis, vasilis@fluid.mech.ntua.gr, National Technical University of Athens, School of Mechanical Engineering (Greece)

Abstract

Over the last 20 years wind energy has undergone a significant growth. The installation of new wind farms is increasing globally with an average rate (over the last five years) of 10 percent every year. Current commercial wind turbines (WTs) have diameters that range between 90 to 150 meters and their total height exceeds 200 meters. Manufacturer's ambition points towards even bigger turbines with rotor diameters that within the next decade will reach sizes of about 250m. The above development will consequently lead to larger areas occupied by future wind farms. On the other hand, helicopters often execute low altitude flights following trajectories that cross wind farm areas. Furthermore, helicopters are commonly used as transport mean for maintenance staff transportation missions to distant offshore wind farms (as for example in the North Sea where many wind farms have been deployed over the last years). It is therefore foreseen that in the coming years the possibility for a helicopter to fly in interaction with a wind turbine wake will increase. Lack of previous experience or evidence renders safety checks necessary. In this respect of particular significance is to know whether safe passage through or in strong interaction with the wake of an operating wind turbine is possible or in such occasion the turbine should be shutdown. In the present paper, the aerodynamic interaction of a helicopter main rotor with a wind turbine wake is analyzed on the basis of free wake vortex analysis. Helicopter forward flight crossings of wind turbine wakes are simulated using different wake flow models.

1. INTRODUCTION

In wind farm environments complex wake disturbances develop encompassing non-uniform wind velocities (sometimes dominated by the interaction of multiple wakes), increased turbulence levels and concentrated vortices trailed by the rotating blades, which produce a highly unsteady flow field. The interaction of the above complex flow field with a helicopter rotor has not been studied in detail. The existing literature is quite limited [1]. Moreover, international regulations concerning the above flight conditions have not been yet developed. Recognition of the importance of the problem and the lack of relevant literature on the topic have led GARTEUR to the definition of a specific action group on this topic (AG-23) [2]. The work presented in the paper is performed in the context of the above group.

The aim of the present paper is the numerical assessment of the aerodynamic loads of a helicopter main rotor, executing flight in interaction with the wake of large multi megawatt turbine. The analysis is performed using the in-house code GenUVP [3]. GENUVP is a potential flow solver combining a panel representation of the rotor blades with a free vortex particles representation of the wake. A particle mesh approach based on the solution of Poisson equation for the vector potential is applied for the wake convection [4]. The vorticity of the wake vortex particles is first projected on a grid and then Poisson equation is solved using a fast Fourier transformation solver.

The work is divided in three parts. In the first part the wake of a WT is simulated and analyzed. It is essential for the understanding of the physics of the above discussed interactional phenomena to obtain a good representation and characterization of the wake of the WT (temporal and spatial representation of the wake deficit, vorticity distribution within the wake). The wake of the NREL 5MW WT [5] is simulated at the rated wind speed (11.4m/s). Wake simulations are performed using two different methods of varying complexity. The first is a prescribed wake, lifting line method, while the second is the free wake vortex particle method employed in GENUVP code. Identification

Presented at 44th European Rotorcraft Forum, Delft, The Netherlands, 19-20 September, 2018

of the interactional phenomena is easier through the prescribed wake analysis, as the position of the trailed vortices is fixed in space. Yet, the free wake approach accounts better for the wake dynamics. Wake velocities time series are recorded over a fixed grid in space both for uniform and turbulent wind conditions.

In the second part, the aerodynamic loads of the BO105 main rotor flying through the above simulated flow fields are calculated and compared on the basis of a one-way interaction, within which the helicopter rotor is affected by the WT wake but not the other way around. Simulations of the helicopter main rotor are performed using the free wake GENUVP code.

In the last part of the paper the effect on the main rotor control angles is analyzed through a simplified quasi-static trim procedure. The main rotor of the BO105 is trimmed for steady level flight at different positions inside the wake of the turbine. Although the time scales of the actual crossing of the wake are not that long to safely assume steady flight conditions, a rough indication of the required control input by the pilot can be obtained.

2. FORMULATION OF THE METHOD

1.1 The flow solver

For the modelling of the flow, GenUVP code combines a panel method [3] with a vortex particle representation of the wake [6], [7]. The theoretical backbone of the method is Helmholtz's decomposition theorem[11] according to which any flow-field $\vec{u}$ can be decomposed into a potential and a vortical part. The potential part $\vec{u}_{solid} = \nabla\phi$ is associated with the presence of the solid boundaries (blades and/or obstacles) in the flow whereas the vortical part $\vec{u}_{wake} = \nabla \times \vec{\psi}$ is associated with the wake or the free vorticity $\vec{\omega}$. By ϕ and $\vec{\psi}$ the scalar and the vector potentials of the flow are denoted satisfying the field equations:

$$\nabla^2\phi = \nabla\vec{u} \equiv \Delta \quad (1)$$

and

$$\nabla^2\vec{\psi} = -\nabla \times \vec{u} \equiv -\vec{\omega} \quad (2)$$

Green's theorem provides integral representations for both parts which in the case of an inviscid and incompressible flow take the following form:

$$\vec{u}_{solid}(\vec{x};t) = \int_{S(t)} \frac{(\sigma \cdot + \vec{\gamma}\times)\vec{r}}{4\pi\vec{r}^3} dS(\vec{y}) \quad (3)$$

$$\vec{u}_{wake}(\vec{x};t) = \int_{D_\omega(t)} \frac{\vec{\omega}(\vec{y};t)\times\vec{r}}{4\pi\vec{r}^3} dD(\vec{y})$$

In (3) $\vec{r} = \vec{x} - \vec{y}$, $D_\omega(t)$ denotes the region covered by the wake, $S(t)$ denotes collectively the solid boundaries and $\sigma, \vec{\gamma}$ denote the surface source and vorticity distributions associated with the normal and tangent to S velocity components. By construction they both vanish at infinity so the velocity at infinity $\vec{u}_{ext}$ must be added in order to form $\vec{u}$.

Based on the above kinematic formulation, the flow equations to be satisfied are:

1. The no-penetration boundary condition: $\vec{u}\cdot\vec{n} = \vec{U}_S \cdot \vec{n}$ where $\vec{U}_S$ denotes the body velocity. $\vec{U}_S$ will include the rotational speed, the speed induced by the pitch control as well as the deformation velocity of flexible blades.
2. The vorticity emission condition also known as Kutta condition. It is applied on the solid surface at predefined lines such as the trailing edge or blade tips; wherefrom the bound vorticity is released continuously in the free flow so as to form the wake. It imposes zero pressure jump across the wake at the emission line.
3. The Helmholtz equations, i.e. the momentum equations written with respect to vorticity.

In potential theory wakes are introduced as material surfaces carrying surface vorticity $\vec{\gamma}$. Existing wake models differ on the choice of elements to describe the wake but most importantly on whether or not they assume connectivity among these elements. Connectivity is necessary in order to satisfy the fundamental requirement that vorticity is div free or else that the vorticity lines in the wake are either closed or they start and end on a solid boundary or at infinity. These requirements are by construction fulfilled when the wake is formed by means of vortex filaments or is retained as a surface. Connectivity however can generate numerical problems when the wake is excessively deformed or interacts with solid bodies as in the present case. In order to bypass this problem, GenUVP uses freely moving vortex blobs. They are 3D point vortices equipped with a core. Vortex blobs are generated at every time step in a two-steps procedure. First the wake is released in the form of surface vorticity. It is in this form that the no-penetration and Kutta conditions are satisfied. Then the convection step is carried out during which surface vorticity is integrated and transformed into vortex blobs defined by their intensity $\vec{\Omega}_P$, their position $\vec{Z}_P$ and their core size ε_P :

Presented at 44th European Rotorcraft Forum, Delft, The Netherlands, 19-20 September, 2018

(4) $$\vec{\omega}(\vec{x};t) \cong \sum_P \vec{\Omega}_P(t)\ \zeta_\varepsilon(\vec{x}-\vec{Z}_P(t))$$

where ζ_ε is the cut-off or distribution function defined over the core. GenUVP uses a cubic exponential function[12] which results in the following velocity representation:

(5) $$\vec{u}_{wake}(\vec{x};t) = \sum_P \frac{\vec{\Omega}_P(t)\times\vec{r}_P}{4\pi r^3}(1-\exp(r^3/\varepsilon^3)$$

where $\vec{r}_P = \vec{x} - \vec{Z}_P$.

The integration satisfies the basic invariant properties of fluid flows:

(6) $$\vec{\Omega}_P(t) = \int_{D_P} \vec{\omega}(\vec{y};t)dD,$$
$$\vec{\Omega}_P(t)\times\vec{Z}_P(t) = \int_{D_P} \vec{\omega}(\vec{y};t)\times\vec{y}\,dD$$

while $\vec{\Omega}_P$ and $\vec{Z}_P$ are determined by integrating in time the corresponding evolution equations:

(7) $$\frac{d\vec{Z}_p(t)}{dt} = \vec{u}(\vec{Z}_p;t), \quad \frac{d\vec{\Omega}_p(t)}{dt} = \left(\vec{\Omega}_p(t)\nabla\right)\vec{u}(\vec{Z}_p;t)$$

Being unconnected, vortex blobs will generate a vorticity field which will eventually violate in time the div free requirement. There are two methods to correct this error: (a) either by remeshing or (b) by using the Particle-Mesh method. Fortunately, the Particle-Mesh method offers additionally a substantial reduction of computational cost and it has been implemented in GenUVP. The vorticity of the wake vortex particles is first projected on a Cartesian grid and then the Poisson equation $\nabla^2\vec{\psi} = -\vec{\omega}$ is solved over the same grid by means of a fast Fourier transformation solver [4]. Then $\vec{u}_{wake} = \nabla\times\vec{\psi}$ and its derivatives appearing in (7) are calculated through finite differences.

3. RESULTS

The results presented in the paper concern i) the analysis of the wake flow of the NREL 5 MW WT, ii) the analysis of the effect of two WT wake flow models on the aerodynamic loads of the BO105 helicopter (forces and moments) and finally, iii) the analysis of the effect of the turbine wake on the controls of the main rotor for steady forward level flight conditions.

3.1. The NREL 5MW Wind Turbine wake

In this section, the WT wake is numerically analyzed. Simulations are performed for the NREL 5 MW turbine, a paper case turbine commonly employed in WT related numerical studies. In the analyses two wake models are considered, i) a simple model based on a lifting line approach, in which the wake is simulated by vortex filaments of prescribed geometry (see figure 1) ii) a more elaborate model based on a lifting surface representation of the blades and unsteady free vortex particle representation of the wake as shown in figure 5. Simulations are performed for the WT operating at the rated wind conditions as shown in table 1.

Table 1 Main geometric and operational characteristics of the reference 5 MW turbine.

Power P (MW)	5
Diameter D (m)	63
Hub height (m)	89
Rated wind speed U (m/s)	11.4
Nominal rotational speed (rad/s)	1.267
Pitch angle at nominal wind velocity (degrees)	0

In both simulation methods the free flow is considered to be uniform. A global, inertial coordinate system is defined that has its origin at the bottom of the tower of the turbine (see Figure 1). The y axis of the system is parallel to the ground and points in the direction of the wind (in case of axial wind conditions), the z axis is vertical and points upwards and the x axis is perpendicular to the other two and points in the direction of the helicopter flight (when the helicopter crosses the wake perpendicular to the direction of the wind). The flow components U, V and W are defined with respect to above described system. Flow field results of the above discussed two methods are presented in the sequel, at the downstream from the WT rotor plane position of two diameters.

3.1.1 The lifting line case

In the lifting-line method the wake is composed by a series of vortex filament spirals trailed from different locations (grid points on the blades) all along the span of the three blades. The pitch of each spiral emanating from a different radial positions is converged during the lifting-line simulations and is kept constant throughout the

Presented at 44th European Rotorcraft Forum, Delft, The Netherlands, 19-20 September, 2018

simulation. In this connection time invariant, axi-symmetric, steady state conditions are simulated.

In Figure 2 - Figure 4, the three velocity components contours (according to the previously defined co-ordinate system) are shown over a wake cross section plane placed two diameters downstream of the rotor plane.

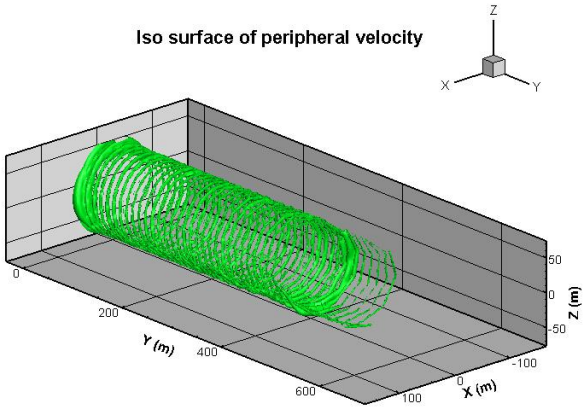

Figure 1 Representation of the wake vorticies in lifting line method.

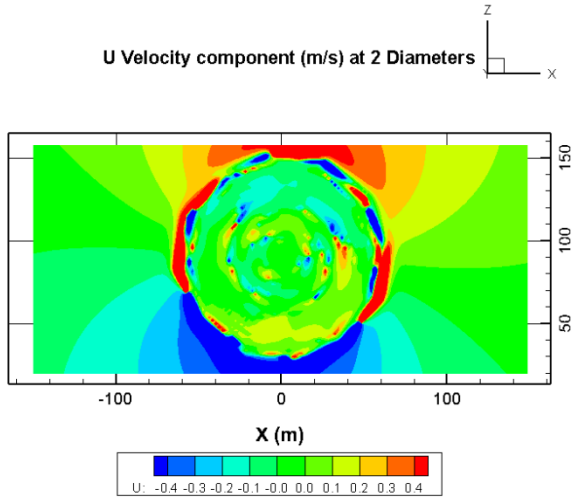

Figure 2 Lifting Line method - U Velocity component.

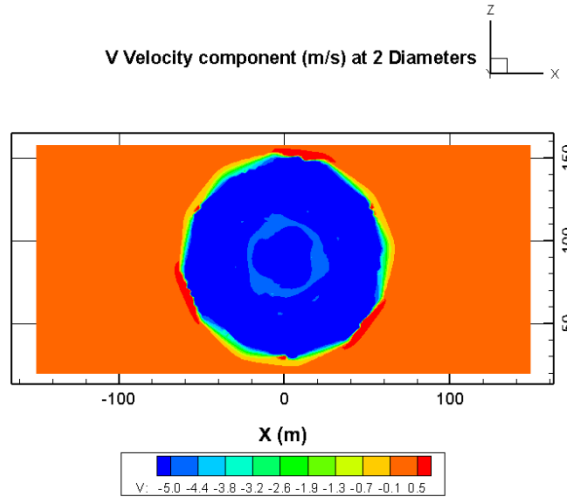

Figure 3 Lifting Line method - V Velocity deficit (flow velocity minus free wind speed of 11.4m/s).

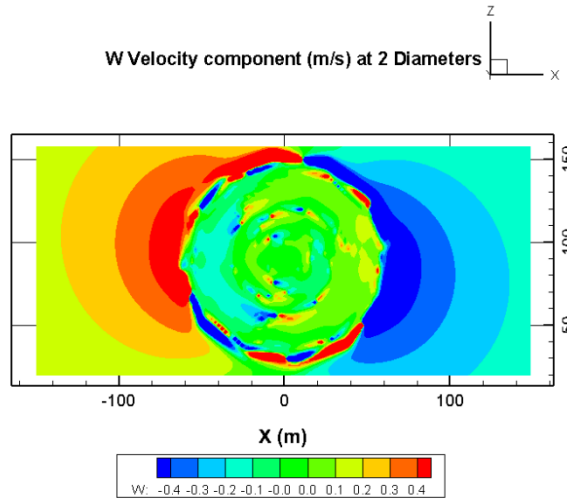

Figure 4 Lifting Line method - W Velocity component.

Especially for the V component, the flow deficit is presented. This is defined as the flow velocity minus the upstream free wind speed (11.4m/s in the present simulation). As seen in Figure 3 an almost constant deficit (V velocity component) of about 5 m/s is obtained within the rotor disk area. Outside the rotor disk area, the deficit is almost zero and therefore the flow is almost undisturbed in the axial direction. The position of the blade tip vortices is indicated on the contour plot by the red spots of the accelerating flow (appearing with a phase shift of 120^{o}). It is noted that the vortex filament system remains fixed throughout the lifting line simulation and therefore the exact location of the blade tip vortices depends on the azimuth position of the blades and the downstream distance

Presented at 44th European Rotorcraft Forum, Delft, The Netherlands, 19-20 September, 2018

of the cross section plane over which velocities are recorded (two diameters in the present simulation). In U and W contour plots (Figure 2 and Figure 4 respectively) the swirling component of the induced velocity is depicted. Anti-clockwise (opposite to the direction of the rotor rotation) rotational (in-plane) flow becomes significant outside the rotor disk area. It appears as high U velocity component (horizontal flow) in the vicinity of 0º/180º azimuthal position and high velocity W component (vertical flow) in the vicinity of 90º/270º position (0º azimuth is the 12 o' clock position). It is noted that as in the case of the axial flow, the azimuthal position of the high in-plane velocity patterns depends on the initial azimuth of the blades (which remains fixed in the lifting line simulation) and the downstream distance of the cross section plane.

3.1.2 The free vortex particle wake case

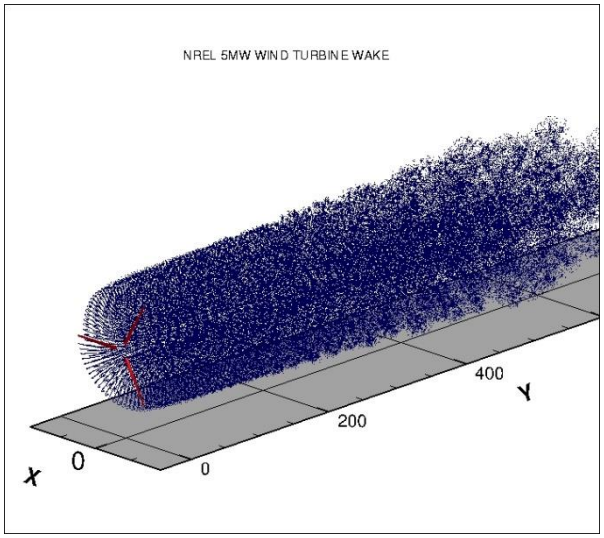

Figure 5 GenUVP (vortex particle representation)

The main advantage of the lifting line simulation is that it is cost effective (one simulation runs in less than a minute) and that the position of the wake vortices is fixed and known. Thereby, interactional phenomena can be easily identified and analysed. The disadvantage of this approach is that the location of the vortices remains frozen and therefore the reproduced flow field is time invariant. Furthermore, wake deformation is omitted in the lifting line simulation. In order to overcome the above limitation an unsteady free wake simulation is performed using the in-house free wake code GENUVP. The free wake pattern of the above simulations at the wind velocity of 11.4m/s is shown in Figure 5.

In Figure 6 – Figure 8, the three velocity components flow patterns are shown over a wake cross section plane placed two diameters downstream of the rotor plane. It is noted that in this case the presented flow fields are averaged over several periods of the simulation. In order to indicate the unsteady character of the predicted flow the sdv plot is shown for V velocity component (see figure 7). It is clear that the unsteady effect is taking place only at the vortex rings that are created near tip and root vortices. Although, the sdv is shown only for one velocity component, the same deviation levels are also present for the other two components (U, W). The 1 m/s of deviation near the rings has not a significant impact on flight velocity and deficit, but makes great change in W velocity component and it is more likely to change the flow filed and therefore to see non-symmetrical results.

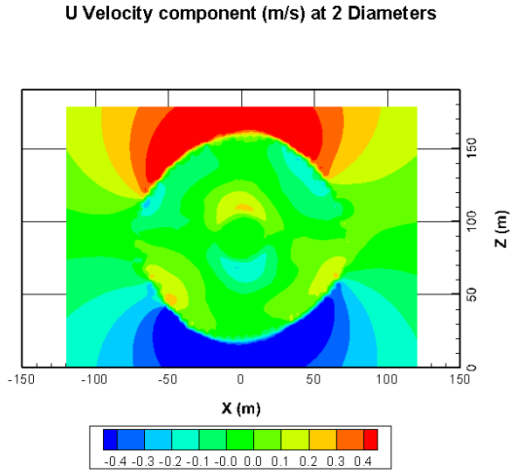

Figure 6 Vortex particle method - U velocity component

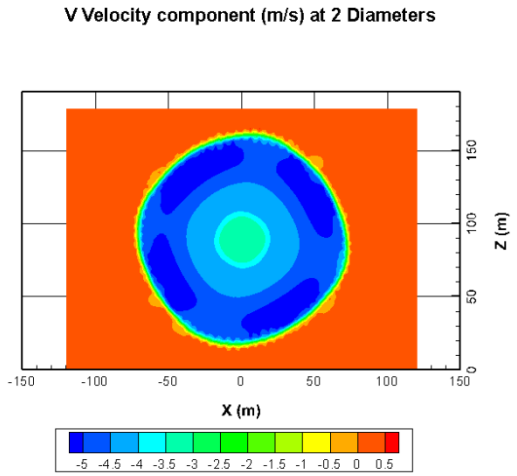

Presented at 44th European Rotorcraft Forum, Delft, The Netherlands, 19-20 September, 2018

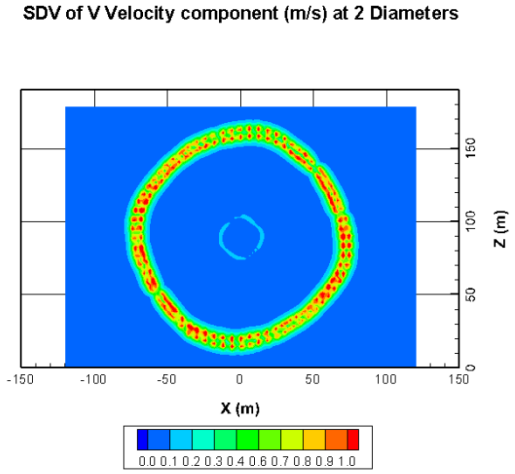

Figure 7 Vortex particle method - V velocity component and standard deviation

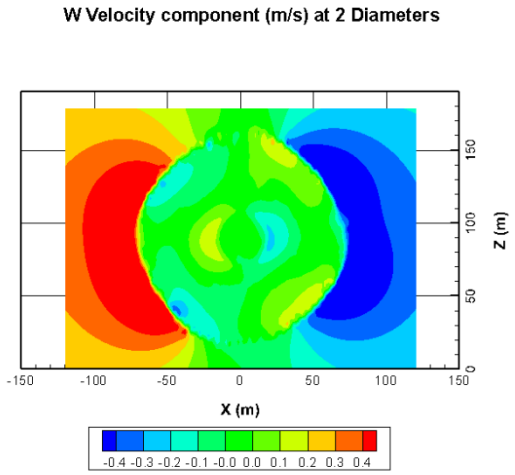

Figure 8 Vortex particle method - W velocity component

Comparison of the results of the free wake simulation against those of the lifting line analysis indicates that in the free wake simulation the patterns of high in-plane velocities appear exactly at the azimuthal positions of 0º/180º for the U component and at 90º/270º for the W component, which stems from the averaging performed on the velocities. Moreover, a less constant deficit is obtained within the rotor disk area. This is due to the fact that in the free wake simulation the rotor blades start at 20% radius (root vortex) and therefore the blockage effect by the inner part of the rotor is missing. Otherwise, the two methods predict similar flow patterns at least in qualitative terms.

3.1.3 Comparison of wake velocities predicted by the two methods

A closer comparison of the results of the two methods is performed in Figure 9.The velocity components predicted by the two methods are compared at the downstream distance of two diameters for a constant height of z=90m (rotor hub height). As discussed in the previous sections, overall, the two methods give similar velocity results. The lifting line method predicts higher values of the V component deficit. Firstly, because the lifting line method predicts slightly higher thrust at the wind velocity of 11.4m/s and secondly because the lifting line method omits expansion of the wake. As seen in the V component plot the radial extend of the wake deficit region is about 15-20% higher in the free wake calculation. Moreover, the velocity deficit rapidly decreases towards the rotor hub in the free wake simulation, which, as already discussed is due to the fact that the inner part of the blade is not taken into account in the simulation. The U component has almost zero mean value in both simulations. The peaks appearing in the lifting line results are due to the random crossing of wake filaments. Such peaks do not appear in the free wake analysis since the velocity results of the free wake simulation have been averaged over several periods. In the W component, an upwash velocity builds up as the WT rotor wake region is approached from negative x values. Within the rotor disk area, the W component is almost zero while at positive x values outside the rotor disk area an almost symmetric downwash is obtained which exponentially decreases as we move away from the rotor disk.

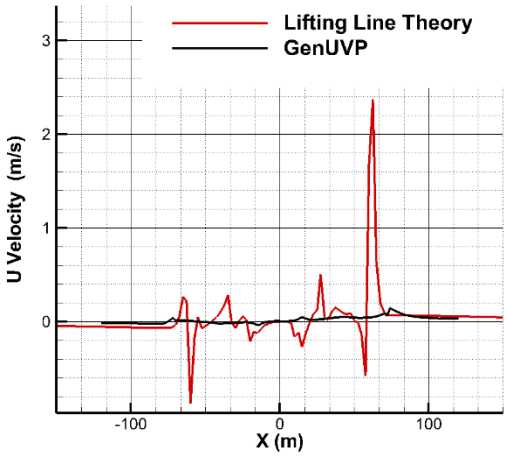

Presented at 44th European Rotorcraft Forum, Delft, The Netherlands, 19-20 September, 2018

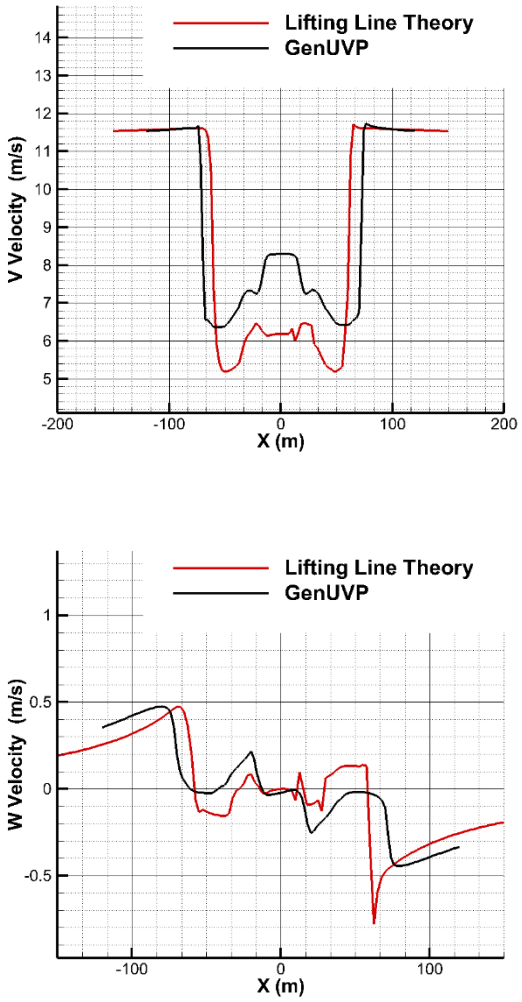

Figure 9 Comparison of the velocities predicted by the lifitng line method against those of the free wake method at two diameters distance from the wind turbine along a line parallel to the ground at a heigh z=90m (hub height).

3.2. Effect of WT wake interaction on BO105 main rotor loads.

Table 2 Level flight main rotor's trim varialbes and attitudes

Collective pitch	5.8 deg
Cyclic pitch (sin)	2 deg
Cyclic pitch (cos)	-1 deg
Pitch attitude	1.6 deg
Roll Attitude	-0.7 deg

In the present section, the effect of the WT wake on the loads of a helicopter main rotor is investigated. The main rotor of a helicopter, which executes level flight perpendicular to a cluster of WTs, encounters strong side winds the magnitude of which depends on the wind velocity within the wind farm. Furthermore, the magnitude of the side wind changes (decrease) as the helicopter crosses the wake region of a turbine. Therefore, as a first step in our analysis we only consider the effect of different magnitudes of side wind on the main rotor loads. Next, the complete wake inflow velocity is considered. This in addition includes significant upwash/downwash flow components, which directly affect the angle of attack of the rotor inflow. All the cases presented in this section concern forward steady flight with a flight speed of 30 m/s. The trim variables of the main rotor and the attitudes are set to those reported in Table 2 which are those corresponding to a helicopter performing level flight with zero side wind. The direction of the helicopter flight is along the x axis of the inertial system (perpendicular to the direction of the incoming wind). The helicopter, as it crosses the wake, moves from negative x values towards positive x values.

The main assumptions made in the analyses that follows in sections 3.2.1 and 3.2.2 are:

- The main rotor is only considered in the analysis of the helicopter and it is simulated using the free wake code GENUVP
- There is a one-way effect of the WT wake on the main rotor
- The helicopter performs steady level flight independent of the changes in the inflow
- Trim variables and attitudes remain fixed throughout the simulations.

3.2.1 The effect of the side winds

In the process of understanding the effect of the different inflow components, first simulations are performed considering only the side wind component. Simulations concern forward steady flight with different percentages (with respect to the helicopter flight speed) of side wind.

Figure 10 and Figure 11 present the ratio of the main rotor forces and moments with respect to the corresponding forces and moments of the reference zero side wind case, as functions of the side wind. In Figure 10 it is seen that the effect of the side wind on the lift force Fz is negligible. A slight increase of about 1% is noted for side winds that exceed 40%. On the other hand, the effect on the side force Fy and thrust force Fx is quite

Presented at 44th European Rotorcraft Forum, Delft, The Netherlands, 19-20 September, 2018

significant. The force in the flight direction decreases by ~25% for 50% side wind values. The main effect is seen in the side force Fy which exhibits a steep reduction with increasing side wind. It is also noted that beyond 47% side winds the side force changes direction. The roll moment Mx shown in Figure 11 presents similar behaviour as the side force Fy. In particular, as the side wind increases the roll moment Mx decreases and changes direction for side winds higher than 40%. On the contrary, the pitching moment My increases and reaches values 2.5 times higher than those of the reference, zero side wind case. The change in the main rotor moments indicates that when a helicopter flies from a high side wind region towards a lower side wind region (as it happens when a rotor crosses the wake of a WT) there is a tendency to turn its nose down and to roll and drift towards the direction of the wind.

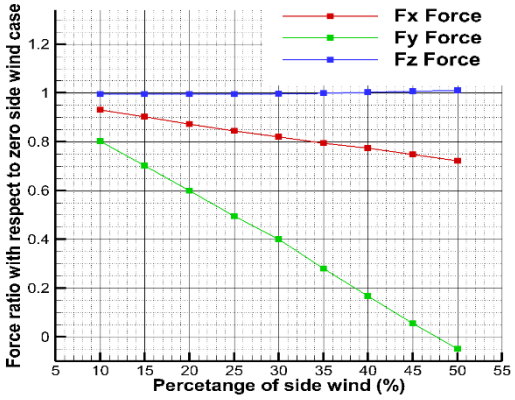

Figure 10 Main rotor hub forces ratio with respect to zero side wind scenario as function of the side wind.

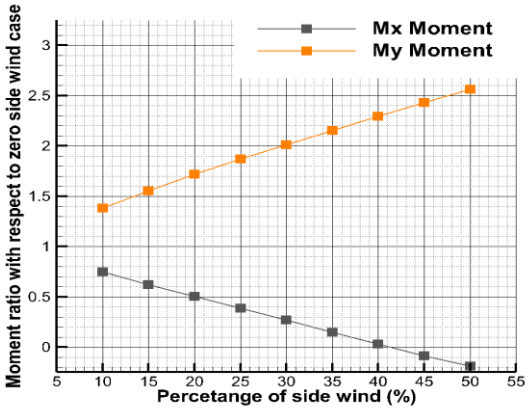

Figure 11 Main rotor hub moments ratio with respect to zero side wind scenario as function of the side wind.

3.2.2 Flying across a wind turbine wake

In the present section, the main rotor loads are analysed in the case that the helicopter crosses perpendicularly the wake of the NREL 5 MW turbine at a downstream distance of two diameters from the WT rotor plane. The wake flow velocities presented in section 3.1 are considered in the analysis. Simulations are performed for both inflow fields namely the lifting line and the free wake flow fields.

In connection to the results presented in the previous section, it is important to note that outside the WT wake deficit region, the side wind is 38% of the flight speed (see Figure 9), while inside the deficit region the side wind decreases and ranges between 20% and 25% of the flight speed. The mean load levels obtained as the rotor flies across the wake are highly correlated to those presented in Figure 10 and Figure 11 as the helicopter inflow is dominated by the side wind. Variations around the above levels are mainly due to the induced wake upwash or downwash velocities.

In Figure 12 – Figure 14 the main rotor loads predicted by GENUVP are compared for the two flow fields (lifting line and free wake) in the case of level flight at a height of z=90m (hub height level) It is noted that quite similar load results are obtained for both flow fields. The physical presence of the WT trailed vortices does not seem to have a significant effect on the loads. The loads are mainly affected by the average flow field (wake deficit and wake induced upwash and downwash)

In particular:

- The Fz force (see figure 12) is mainly affected by the W flow component. As earlier discussed, the side wind has negligible effect on Fz force. The induced upwash velocity (see Figure 9), as the rotor approaches the wake (from negative x values), increases the angles of attack of the rotor leading to 3-5% higher Fz force while the induced downwash when exiting the wake region leads to 2% lower Fz force. Within the wake region Fz remains almost unaffected.
- The rolling moment Mx (see figure 13) is mainly affected by the side wind. In agreement with the results of figure 11 the rolling moment is lower outside the wake region (ratio of 0.1 with respect to the reference) and higher within the wake region (ratio 0.4-0.5 with respect to the reference). The slight asymmetry observed between the left and right edge of the wake is due to the secondary effect of the W component.

Presented at 44th European Rotorcraft Forum, Delft, The Netherlands, 19-20 September, 2018

- The pitching moment My presents similar behaviour as that of the rolling moment Mx (see figure 14). Again, because of the side wind, higher pitching moments are obtained outside the wake region (ratio 2.2-2.5 with respect to the reference) and lower within the rotor disk area (ratio 1.8-2 with respect to the reference case). The results are again in qualitative agreement with the results presented in figure 11. The asymmetry observed between the left and right edge of the wake is higher on My as compared to Mx, indicating that the effect of the W component is higher on the pitching moment.

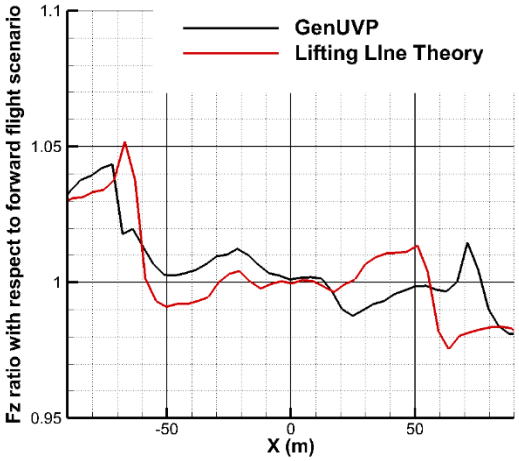

Figure 12 Lift force Fz ratio - comparison of the two wake flow fields, flight height z=90m.

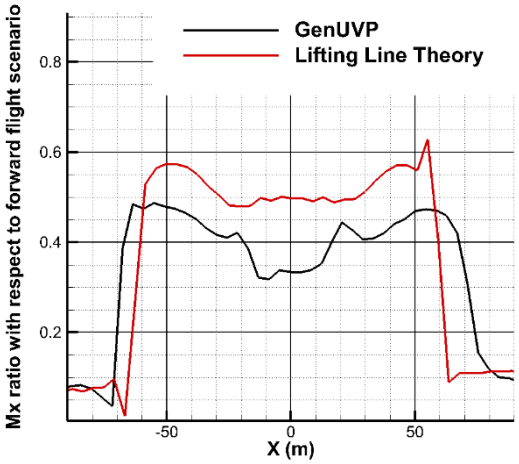

Figure 13 Rolling moment Mx ratio - comparison of the two wake flow fields, flight height z=90m.

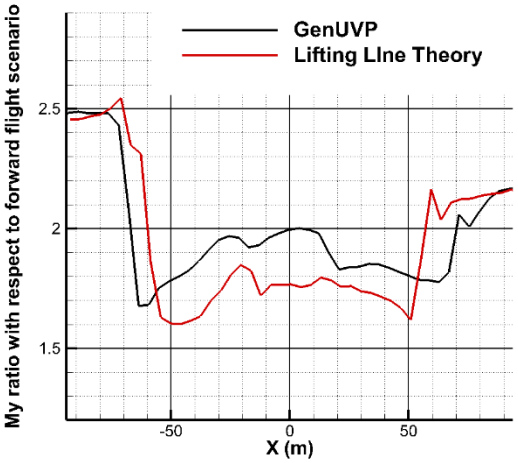

Figure 14 Pitching moment My ratio - comparison of the two wake flow fields, flight height z=90m.

In Figure 15, a pattern of the main rotor wake is shown as the helicopter crosses the turbine wake. The box represents the dimensions of the grid over which wake induced velocities have been recorded.

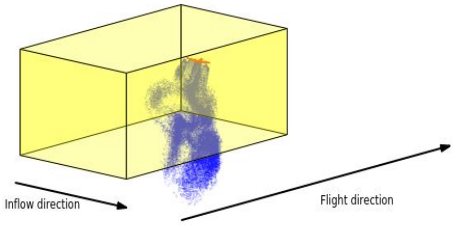

Figure 15 Main rotor's wake pattern.

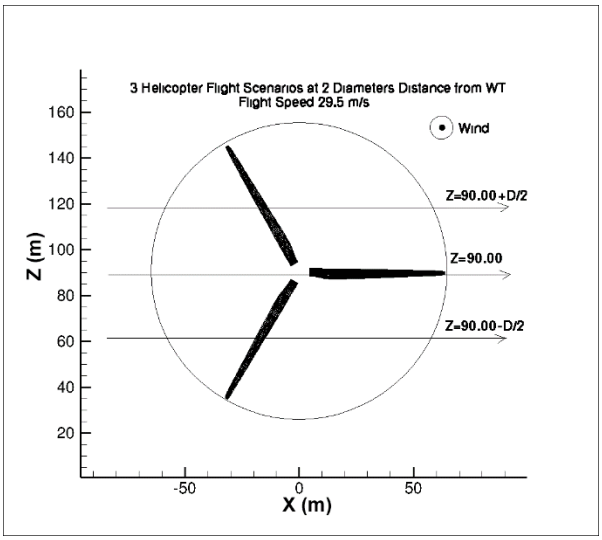

Figure 16 Heights for which wake crossing simulations are performed.

Presented at 44th European Rotorcraft Forum, Delft, The Netherlands, 19-20 September, 2018

Next, wake crossing simulations at different flight heights are performed using the free wake GENUVP code. Two additional simulations are performed at z=60 m and z=120 m. The load results obtained for the three different heights are compared in Figure 17 – Figure 19.

The results obtained for the three different heights are similar in qualitative terms. As in the case of the hub height load variations along the flight path are dictated by the effect of the side wind and the effect of the downwash/upwash velocities. Small differences are noted especially close to the wake edges (when the rotor enters or exits the wake region), which are all related to instant and random crossings of the WT rotor tip vortices. These differences are more pronounced in the rolling moment Mx. As seen in Figure 18, a down-shoot is noted in the Mx moment at the flight height of z=60m, when the rotor enters the wake while an overshoot is obtained at z=120m when the rotor exits the wake. Smoother variation is obtained at the flight height of z=90m. The closest agreement between the three heights is obtained for the pitching moment My.

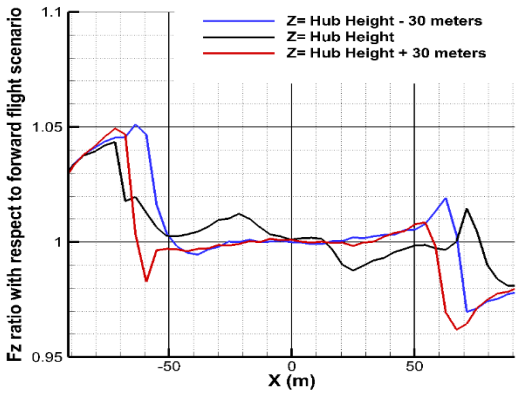

Figure 17 Lift force Fz ratio – load comparison at three different flight heights.

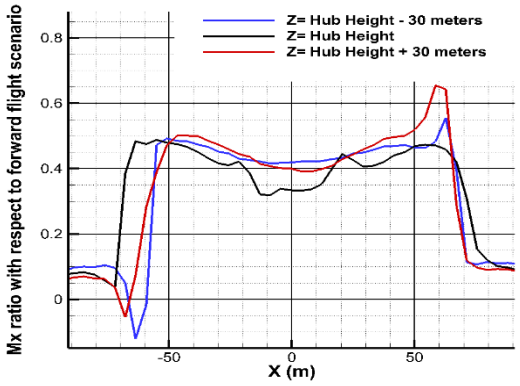

Figure 18 Rolling moment Mx ratio – load comparison at three different flight heights.

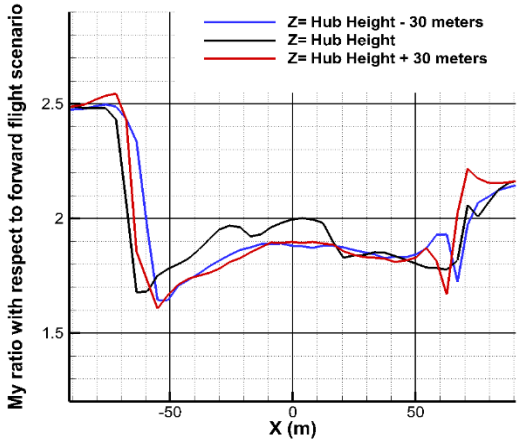

Figure 19 Pitching moment My ratio – load comparison at three different flight heights.

3.3. Effect of WT wake interaction on BO105 main rotor control angles

In the present section, the effect of the helicopter interaction with the wake of a WT on the control angles of the main rotor is analysed. In this connection a simplified quasi-static trim procedure is performed at different positions along the flight path of a helicopter crossing the wake of a WT.

The simplified trim method is based on the following assumptions.

- Rolling Mx and Pitching My with respect to the centre of gravity of the helicopter are set equal to zero
- The lift force Fz is set equal to the weight of the helicopter
- The thrust force Fx is set equal to the drag force of the helicopter
- The side force Fy is set equal to the thrust of the tail rotor which is assumed to be such that it always counter acts the rotation moment Mz of the main rotor.

As the load patterns of the flights at different altitudes presented in the previous section exhibited very similar behaviour, in the present section the analysis of the effect on control angles is performed for two different altitudes, one at z=30m and a second at z=150. The reference flight case at the level of the WT hub (z=90m) is also considered. The two new cases correspond to flights parallel to the blade tip vortices close to the lower (z=30m) and upper edges (z=150m) of the turbine wake.

Presented at 44th European Rotorcraft Forum, Delft, The Netherlands, 19-20 September, 2018

The flow components for the two new cases are shown in Figure 20. Comparing the velocities of the new cases against those of Figure 9 (flight at the hub height), it is seen that a narrower deficit is obtained when flying at z=30m and 150m. Obviously, maximum deficit extent is obtained when the wake crossing is along the diameter of the wake, which is at the level z=90m. At the hub height, the lateral component of the flow U is almost zero all along the flight path while in the two new cases there is a significant lateral flow component of opposite sign but similar shape, which is due to the wake swirling. Within the wake region the lateral wind component U is almost zero while it takes its maximum absolute value right at the edge of the wake on both sides (left and right). The U component exponentially decays as we move away from the wake edges on both sides. Vertical velocity component W of similar shape is obtained for both flight paths (z=30m and 150m). An upwash velocity builds up as the wake region is approached from negative x values. When the wake region is crossed a sudden change of the velocity sign occurs (downwash velocities are obtained inside the wake region) but as we move along the wake region W velocity builds up again and obtains positive values before we reach the right edge. Again, a sudden change of sign (from upwash to downwash) occurs as the right edge of the wake is crossed. Comparing the W component of the two new cases with the flight case at the hub height they appear to be quite similar especially outside the wake region.

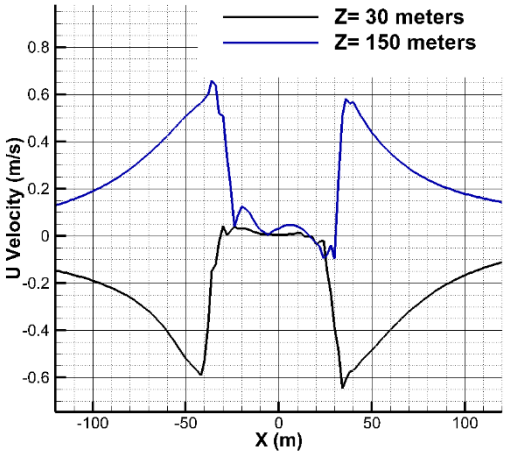

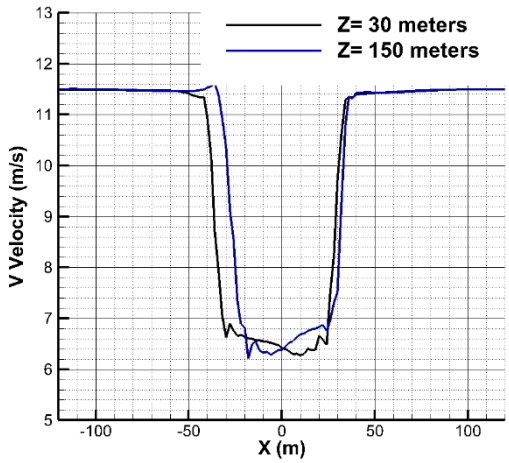

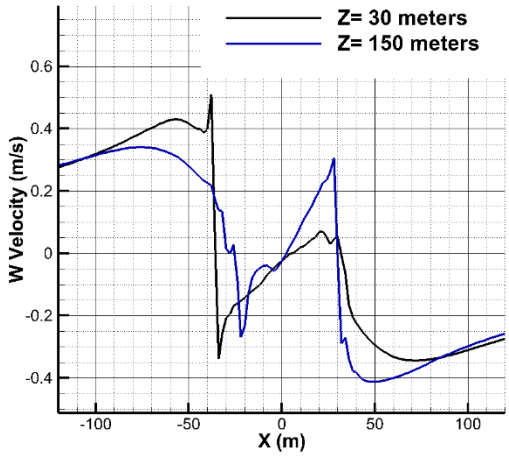

Figure 20 Velocities at 30 and 150 meters above the ground level at two diameters downstream of the wind turbine

In Figure 21 - Figure 23 the collective and cyclic control angles of the three flight cases are compared. It is seen that the collective angle follows a similar pattern in all three cases. The collective angle tends to increase all along the flight path as a result of the decreasing lift (see Figure 14 and Figure 17). The shape of the variation is similar at all flight altitudes. Higher differences are seen in the vicinity of x=-60m and x=60m which are due to the different extent of the wake deficit region of the different flight altitudes. An overall 10% change of the collective angle is obtained. The cyclic sinus pitch angle variation follows closely the shape of the wake deficit. It is therefore dominated by the change of the side wind along the flight path. The shape of the variation is almost symmetric on the two sides of the wake which means that the sinus pitch angle is not affected by the lateral flow component U or the vertical flow component W.

Presented at 44th European Rotorcraft Forum, Delft, The Netherlands, 19-20 September, 2018

The overall change in the cyclic sinus angle is 8%. The shape of the deficit is also followed by the cyclic cosine pitch angle. However, the shape of the variation in the case of the cosine angle is not symmetric between the two sides of the wake which indicates that this angle is affected by the vertical component W of the wind flow. Lower (in absolute value) cosine angles are obtained on the left side which is dominated by upwash velocities as compared to the right side which is dominated by downwash velocities. The overall change in the cosine angle is of the order of 30%.

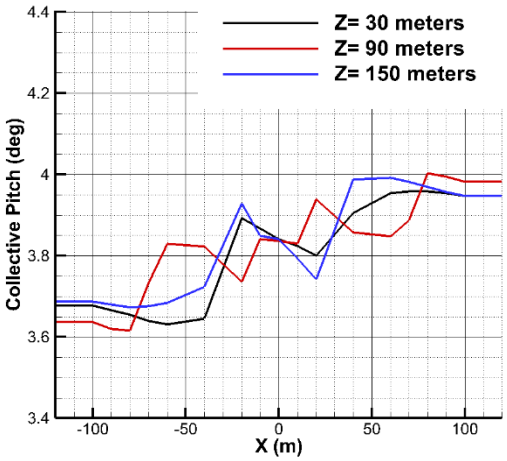

Figure 21 Collective pitch angle

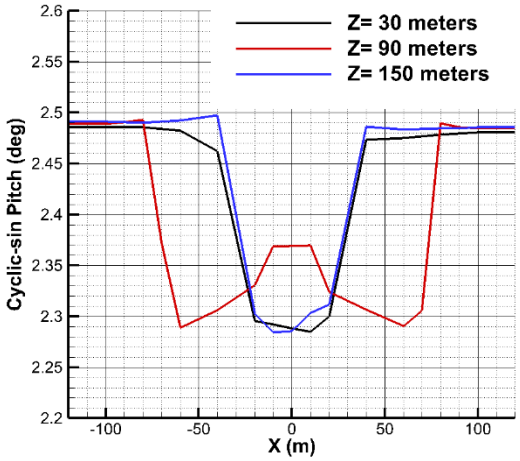

Figure 22 Cyclic-sin pitch angle.

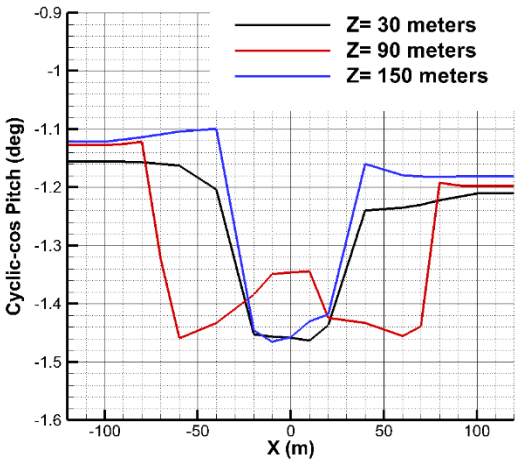

Figure 23 Cyclic-cos pitch angle

4. CONCLUDING REMARKS

In this paper the analysis of the NREL wind turbine wake is performed using two different potential flow models of different complexity (prescribed wake lifting line and unsteady free wake vortex particle). Comparison of predicted flow patterns indicated that both models provide qualitatively similar results. Furthermore, it is identified that the main characteristics of the wake flow that can affect the flight of a helicopter across it, are the significant velocity deficit within the wake region and the upwash and downwash flow components developing at the edges of the wake as a result of the wake swirling effect. Main rotor loads are computed for level flights at different altitudes across the wake region and it is shown that the effect of the main rotor interaction with the WT wake is negligible on the lift force but quite significant on the hub moments. While the lift force is mainly affected by the vertical flow component the hub moments are mainly driven by the change in the side wind (wake deficit due to extraction of energy by the rotor). Helicopter flight across the wake of a WT will cause a sudden change in the helicopter attitudes. As the rotor crosses the wake there is a tendency for a nose down pitch and a clockwise roll rotation while the helicopter tends to drift in the direction of the wind due to significant change in the side force. The above changes require significant pilot input in order to maintain level flight with the same flight speed. It is identified that the main effect on pilot's input will be on the cyclic cosine angle which across the wake needs to be changed by about 30%.

Presented at 44th European Rotorcraft Forum, Delft, The Netherlands, 19-20 September, 2018

5. REFERENCES

1. van der Wall, B.G., Fischenberg, D., Lehmann, P.H., van der Wall, L.B.: Impact of Wind Energy Rotor Wakes on Fixed-Wing Aircraft and Helicopters, 42nd European Rotorcraft Forum, Lille, France, Sept. 5-8, 2016
2. HC/AG-23: Wind Turbine Wakes and Helicopter Operations, http://www.garteur.org/Action%20Group%20posters/HC_AG-23%20Poster%20v2016.pdf
3. Voutsinas, S. G. (2006). Vortex methods in aeronautics: how to make things work. International Journal of Computational Fluid Dynamics, 20(1), 3-18.
4. Papadakis, G., & Voutsinas, S. G. (2014). In view of accelerating CFD simulations through coupling with vortex particle approximations. In Journal of Physics: Conference Series (Vol. 524, No. 1, p. 012126). IOP Publishing.
5. J. Jonkman. NREL 5 MW baseline wind turbine. Technical report, NREL/NWTC, 1617 Cole Boulevard; Golden, CO 80401-3393, USA, 2005.
6. C. Rehbach, “Calcul d’ecoulements autour d’ailes sans epaisseur avec nappes tourbillonnaires evolutives », Recherche Aerospatiale 2:53-61, 1973.
7. G-H Cottet, P.D. Koumoutsakos, ”Vortex methods: Theory and Practice”, Cambridge University Press, 2000

Presented at 44th European Rotorcraft Forum, Delft, The Netherlands, 19-20 September, 2018